Biogeosciences, 12, 723–738, 2015
www.biogeosciences.net/12/723/2015/
doi:10.5194/bg-12-723-2015

Biogeosciences Open Access

Authigenic apatite and octacalcium phosphate formation due to adsorption–precipitation switching across estuarine salinity gradients

J. F. Oxmann[1] **and L. Schwendenmann**[2]

[1]GEOMAR Helmholtz Centre for Ocean Research Kiel, Marine Biogeochemistry, 24148 Kiel, Germany
[2]School of Environment, The University of Auckland, Auckland 1010, New Zealand

Correspondence to: J. F. Oxmann (joxmann@geomar.de)

Received: 11 May 2014 – Published in Biogeosciences Discuss.: 1 July 2014
Revised: 15 December 2014 – Accepted: 29 December 2014 – Published: 6 February 2015

Abstract. Mechanisms governing phosphorus (P) speciation in coastal sediments remain largely unknown due to the diversity of coastal environments and poor analytical specificity for P phases. We investigated P speciation across salinity gradients comprising diverse ecosystems in a P-enriched estuary. To determine P load effects on P speciation we compared the high P site with a low P site. Octacalcium phosphate (OCP), authigenic apatite (carbonate fluorapatite, CFAP) and detrital apatite (fluorapatite) were quantitated in addition to Al / Fe-bound P (Al / Fe-P) and Ca-bound P (Ca-P). Gradients in sediment pH strongly affected P fractions across ecosystems and independent of the site-specific total P status. We found a pronounced switch from adsorbed Al / Fe-P to mineral Ca-P with decreasing acidity from land to sea. This switch occurred at near-neutral sediment pH and has possibly been enhanced by redox-driven phosphate desorption from iron oxyhydroxides. The seaward decline in Al / Fe-P was counterbalanced by the precipitation of Ca-P. Correspondingly, two location-dependent accumulation mechanisms occurred at the high P site due to the switch, leading to elevated Al / Fe-P at pH < 6.6 (landward; adsorption) and elevated Ca-P at pH > 6.6 (seaward; precipitation). Enhanced Ca-P precipitation by increased P loads was also evident from disproportional accumulation of metastable Ca-P ($Ca\text{-}P_{meta}$) at the high P site. Here, sediments contained on average 6-fold higher $Ca\text{-}P_{meta}$ levels compared with the low P site, although these sediments contained only 2-fold more total Ca-P than the low P sediments. Phosphorus species distributions indicated that these elevated $Ca\text{-}P_{meta}$ levels resulted from transformation of fertilizer-derived Al / Fe-P to OCP and CFAP in nearshore areas. Formation of CFAP as well as its precursor, OCP, results in P retention in coastal zones and can thus lead to substantial inorganic P accumulation in response to anthropogenic P input.

1 Introduction

Desorption and precipitation of phosphate along salinity gradients are influenced by redox potential (Eh) and pH (van Beusekom and de Jonge, 1997). Typically, Eh decreases and pH increases from land to the sea (Clarke, 1985; Huang and Morris, 2005; Sharp et al., 1982). Seawater inundation induces the Eh gradient by limiting oxygen diffusion into the sediment, thereby initiating anaerobic respiration. Sediments regularly inundated by seawater tend to have higher pH values than terrestrial soils because soils naturally acidify due to vegetation-derived inputs (effects of enhanced carbonic acid production, root exudate release, litter decomposition, proton extrusion). Human activities such as N fertilization can also contribute to soil acidification (Fauzi et al., 2014; Hinsinger et al., 2009; Richardson et al., 2009). The acid generated is neutralized downstream by the high alkalinity of seawater.

Changes in pH and Eh facilitate phosphorus (P) desorption from particulate matter and generally account for the non-conservative behaviour of dissolved reactive P during admixing of water along salinity gradients. Particulate P includes a significant amount of inorganic P, which mainly consists of calcium-bound P (Ca-P; detrital and authigenic) and aluminium / iron-bound P (Al / Fe-P). The Al / Fe-P fraction

contains adsorbed inorganic P (Al / Fe-(hydr)oxide-bound P), which can be partly released to solution (e.g. Slomp, 2011). The Al / Fe-P fraction of oxidized, acidic sediment usually comprises relatively large proportions of adsorbed P. Phosphate desorption induced by pH and Eh gradients generally results in progressively decreasing concentrations of the Al / Fe-P from upper to lower intertidal zones (Andrieux-Loyer et al., 2008; Coelho et al., 2004; Mortimer, 1971; Jordan et al., 2008; Paludan and Morris, 1999; Sutula et al., 2004).

Decreasing Eh in sediment from upper to lower zones involve critical levels for reduction of ferric iron compounds (e.g. Gotoh and Patrick, 1974). These critical levels facilitate desorption of Fe-(hydr)oxide-bound P due to less efficient sorption of P by iron in the Fe(II) state compared to the Fe(III) state (Hartzell and Jordan, 2012; Sundareshwar and Morris, 1999). Desorption from metal (hydr)oxides with increasing pH (Oh et al., 1999; Spiteri et al., 2008), on the other hand, is driven by the decreasing surface electrostatic potential with increasing pH (Barrow et al., 1980; Sundareshwar and Morris, 1999). This effect may be partly offset by the increasing proportion of the strongly sorbing divalent phosphate ion (HPO_4^{2-}) with increasing pH until pH 7 ($\sim pK_2$, which decreases with salinity increase; Atlas, 1975). In the alkaline pH range, however, this offset is less pronounced thus allowing stronger desorption (Bolan et al., 2003; Bowden et al., 1980; Haynes, 1982). Similarly, studies on soils attributed desorption with pH to increasing competition between hydroxyl and phosphate ions for sorption sites, or to less sorption sites due to Al hydroxide precipitation (Anjos and Roswell, 1987; Smyth and Sanchez, 1980).

The release of P adsorbed on Al / Fe-(hydr)oxide facilitates Ca-P formation at higher pH (e.g. during early diagenesis in marine sediment; Heggie et al., 1990; Ruttenberg, 2003; Ruttenberg and Berner, 1993; Slomp, 2011). Consequently, desorption at higher pH does not necessarily increase soluble P (van Cappelen and Berner, 1988; Reddy and Sacco, 1981). This agrees with a switch from low phosphate concentrations in equilibrium with adsorbed P at acidic pH to low phosphate concentrations in equilibrium with mineral Ca-P under alkaline conditions (e.g. Murrmann and Peech, 1969). Low equilibrium concentrations under alkaline conditions are a result of the decreasing solubility of Ca-P phases, such as carbonate fluorapatite (CFAP) and octacalcium phosphate (OCP), with increasing pH (Hinsinger, 2001; Murrmann and Peech, 1969). Precipitation of Ca-P may therefore mitigate a desorption-derived P release from sediment (e.g. van Beusekom and de Jonge, 1997). Similarly, Ca-P precipitation is likely to result in the occasionally observed and apparently conflicting decrease of available P by liming to neutral or alkaline pH (Bolan et al., 2003; Haynes, 1982; Naidu et al., 1990). Accordingly, concentrations of Ca-P usually increase seaward as a consequence of enhanced precipitation (Andrieux-Loyer et al., 2008; Coelho et al., 2004; Paludan and Morris, 1999; Sutula et al., 2004).

Authigenic Ca-P is widely dispersed in marine sediment, but its solubility in seawater remains difficult to predict. Because seawater has been proposed as being largely undersaturated or close to saturation with respect to CFAP, both a possible formation or dissolution of CFAP in seawater cannot be entirely excluded at present (Atlas and Pytkowicz, 1977; Baturin, 1981; Bentor, 1980; Faul et al., 2005; Lyons et al., 2011). In contrast, detrital fluorapatite (FAP) is unlikely to dissolve in seawater (Ruttenberg, 1990; Howarth et al., 1995). In addition to the dependence on species-specific saturation states (Atlas, 1975; Gunnars et al., 2004), the occurrence of Ca-P minerals depends on their formation kinetics (Atlas and Pytkowicz, 1977; Gulbrandsen et al., 1984; Gunnars et al., 2004; Jahnke et al., 1983; Schenau et al., 2000; Sheldon, 1981) and inhibitors such as Mg^{2+} ions (Golubev et al., 1999; Gunnars et al., 2004; Martens and Harriss, 1970). In general, the first solid to form is the one which is thermodynamically least favoured (Ostwald step rule; see Morse and Casey, 1988 and Nancollas et al., 1989).

Given slow or inhibited direct nucleation (Golubev et al., 1999; Gunnars et al., 2004; Martens and Harriss, 1970), species of the apatite group may form by transformation of metastable precursors that are less susceptible to inhibitory effects of Mg^{2+} such as OCP (Oxmann, 2014; Oxmann and Schwendenmann, 2014). Precursor phases form more readily (e.g. days to weeks for OCP; Bell and Black, 1970) and can promote successive crystallization until the thermodynamically favoured but kinetically slow apatite formation occurs (ten to some thousand years; Schenau et al., 2000; Jahnke et al., 1983; Gulbrandsen et al., 1984). Several studies presented field and experimental evidence for this mode of apatite formation in sediment systems (Gunnars et al., 2004; Jahnke et al., 1983; Krajewski et al., 1994; Oxmann and Schwendenmann, 2014; Schenau et al., 2000; van Cappellen and Berner, 1988). A systematic comparison of P K-edge XANES (X-ray absorption near-edge structure spectroscopy) fingerprints from reference materials and marine sediment particles also provided evidence for the occurrence of OCP in sediment (Oxmann, 2014). However, despite significant progress in the determination of different matrix-enclosed Ca-P phases, it is not yet clear whether specific conditions at certain locations facilitate successive or direct crystallization of apatite (Slomp, 2011).

Provided more soluble Ca-P minerals such as OCP or less stable CFAP form in coastal environments, these minerals might mirror short-term changes of human alterations to the P cycle. Conversely, sparingly soluble apatite minerals may reflect long-term changes due to slow precipitation. Hence, the proportion of more soluble Ca-P should increase relative to total Ca-P in response to increased P inputs. This human alteration to the solid-phase P speciation may have implications for P fluxes and burial. To better describe P transformations from terrestrial to marine systems and to track the fate of anthropogenic P inputs, we analysed effects on P fractions and species across different ecosystems of a high P

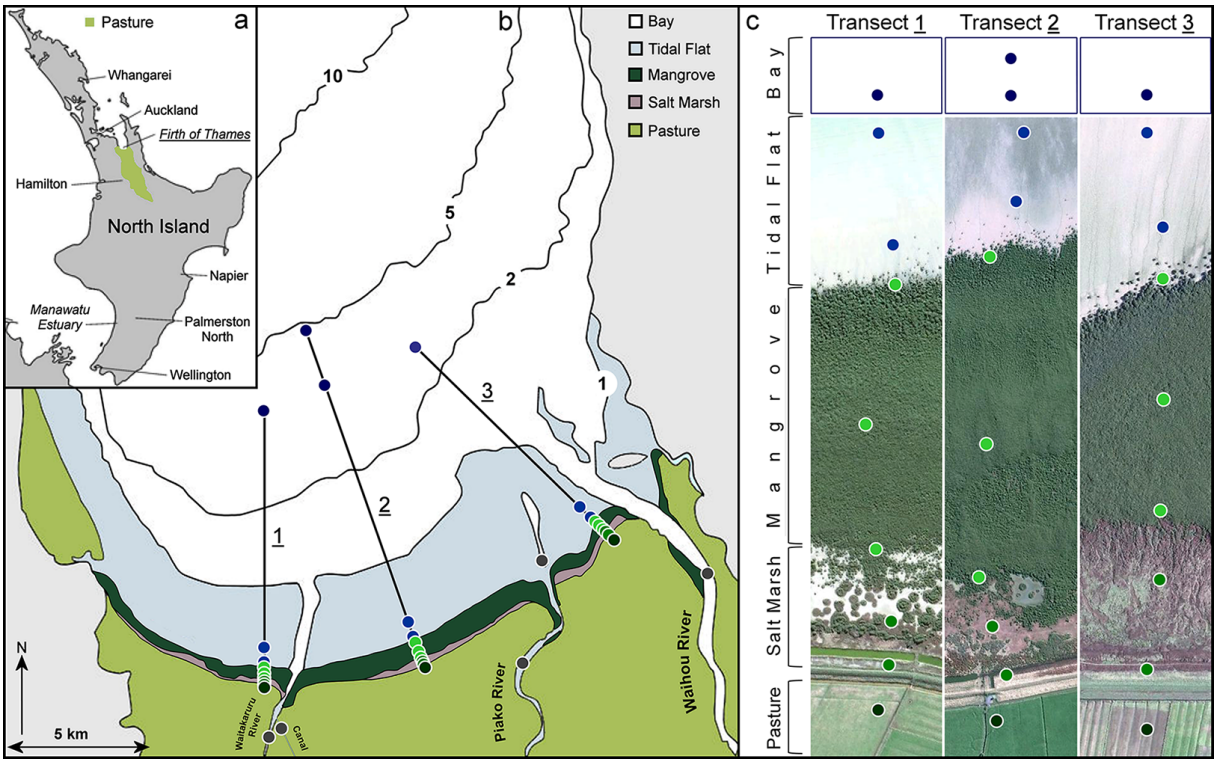

Figure 1. Study area. **(a)** Location of the Firth of Thames, North Island, New Zealand. The area of the catchment area, which is predominantly used for pastoral agriculture (1.3 million ha), is shown in green. **(b)** Firth of Thames transects across different ecosystems. **(c)** Plots ($n = 28$) along transects were located in the following ecosystems: bay (dark blue), tidal flat (blue), mangrove (light green), salt marsh (green) and pasture (dark green). Tidal flat plots close to mangrove forests included mangrove seedlings. Five additional plots were located at rivers (grey). Isolines indicate elevations in metres below mean sea level. Google Earth images for areas from pasture to tidal flat in **(c)**.

site (Firth of Thames, New Zealand). We then compared the findings with results from a low P site (Saigon River delta, Vietnam) to distinguish speciation differences related to increased P loads. Octacalcium phosphate, authigenic apatite and detrital apatite were determined using a recently validated conversion–extraction method (CONVEX; Oxmann and Schwendenmann, 2014).

2 Materials and methods

2.1 Study area, Firth of Thames, New Zealand

The Firth of Thames, a meso-tidal, low-wave energy estuary of the Waikato region rivers Waihou and Piako, is located at the southern end of the Hauraki Gulf (37° S, 175.4° E; Fig. 1). It is the largest shallow marine embayment in New Zealand (800 km^2; < 35 m depth). The tides are semi-diurnal with a spring tide range of 2.8 m and a neap tide range of 2.0 m (Eisma, 1997). The southern shore of the bay (~ 7800 ha) is listed as a wetland of international importance under the Ramsar Convention. The Firth of Thames encompasses large tidal flats (up to 4 km wide) and extensive areas of mangroves (*Avicennia marina* subsp. *australasica*) at the southern end of the embayment (Brownell, 2004). Mangroves have been expanding seawards leading to a 10-fold increase in area since the mid-1900s (Swales et al., 2007). Mangrove expansion has been related to sediment accumulation and nutrient enrichment but may also coincide with climatic conditions (Lovelock et al., 2010; Swales et al., 2007). The upper coastal intertidal zone is covered by salt marshes. Behind the levee ca. 1.3 million ha is used for pastoral agriculture ($\sim$ half of the total area of the Waikato region; Hill and Borman, 2011; Fig. 1a).

2.2 Sampling, field measurements and sample preparation

We established 28 plots along three transects (Fig. 1b, c). Transects extended across the entire tidal inundation gradient and across different ecosystems including bay ($n = 4$), tidal flat ($n = 6$), mangrove ($n = 9$), salt marsh ($n = 6$) and pasture ($n = 3$). Transects were at least 300 m from rivers to exclude areas affected by sediment aeration. Five additional plots were located along rivers. Sediment cores were taken during low tide using a polycarbonate corer (one core per plot; length: 40 cm; diameter: 9 cm). Immediately after core sampling, sediment pH, Eh and temperature were measured

in situ at 0–5, 10–15, 30–35 and 35–40 cm depth intervals. Cores were divided into the following surface, intermediate and deeper sections: 0–5, 10–15, 30–35 and 35–40 cm. Longer core sections reduce vertical variability and were chosen for the relatively coarse vertical sampling because the focus of this study was on geochemical changes along the land–sea continuum. Samples were kept on ice and subsequently frozen until further processing. After thawing roots were removed from the sediment samples. Subsamples were then taken for particle size and salinity analysis. The remaining material was dried, ground and sieved (37 °C; < 300 µm mesh; PM 100; Retsch, Haan, Germany) for P and nitrogen analyses.

Temperature, pH and Eh were measured with a Pt-100 temperature sensor, sulfide resistant SensoLyt SEA/PtA electrodes and pH/Cond340i and pH 3310 mV meters (WTW, Weilheim, Germany). The mV meters were connected to a computer with optoisolators (USB-isolator; Serial: 289554B; Acromag Inc., Wixom, USA) for data visualization and logging (MultiLab pilot; WTW, Weilheim, Germany). Topographic elevation at the plots was measured with a total station (SET530R; Sokkia Co., Atsugi, Japan) relative to a reference point and converted to geo-referenced elevation using a global navigation satellite system (Trimble R8; Trimble Navigation Ltd., Sunnyvale, USA). Inundation duration was calculated from measured elevation above mean sea level and local tide tables (Waikato Regional Council, Hamilton East, New Zealand).

2.3 Sediment analyses

Phosphorus fractions and total P were analysed using three different methods. (i) The relative proportion of more soluble Ca-P was determined by preferential extraction of this fraction using the Morgan test method (Morgan, 1941); (ii) Al / Fe-P and Ca-P fractions were determined by sequential extraction of P after Kurmies (1972); and (iii) total P (TP) was analysed after Andersen (1976) as modified by Ostrofsky (2012). The Morgan test, commonly used to determine available P, preferentially extracts more soluble Ca-P phases using a pH 4.8 buffered acetic acid (see Sect. 4.4). Hence, the term metastable Ca-P ($Ca\text{-}P_{meta}$) is used for Morgan P in this paper. The method of Kurmies includes initial wash steps with KCl / EtOH to eliminate OCP precipitation prior to the alkaline extraction and Na_2SO_4 extractions to avoid readsorption. It therefore provides an accurate means of determining Al / Fe-P and Ca-P using NaOH and H_2SO_4, respectively (Supplement Fig. S2c; steps 2a–3c). Total inorganic P (TIP) was defined as the sum of inorganic P fractions (Ca-P, Al / Fe-P). Organic P was calculated by subtracting TIP from TP.

Octacalcium phosphate, CFAP (authigenic apatite) and FAP (detrital apatite) were quantitated using the CONVEX method (Oxmann and Schwendenmann, 2014). This method employs a conversion procedure by parallel incubation of sediment subsamples at different pH values (approximate pH range 3 to 8) in 0.01 M $CaCl_2$ for differential dissolution of OCP, CFAP and FAP (Fig. S2c). The concentration of OCP, CFAP and FAP is determined by the difference of Ca-P concentrations before and after differential dissolution of OCP, CFAP and FAP, respectively. These Ca-P concentrations are determined by the method of Kurmies. Differential dissolution was verified by standard addition experiments. For these experiments, reference compounds were added to the sediment subsamples before incubation using polyethylene caps loaded with 2 µmol P g^{-1} (ultra-micro balance XP6U; Mettler Toledo GmbH, Greifensee, Switzerland). Reference compounds included OCP, hydroxylapatite (HAP), various CFAP specimens, FAP and biogenic apatite. Methodology, instrumentation and the suite of reference minerals are described in Oxmann and Schwendenmann (2014). CONVEX analysis was conducted for seven sediment samples (differential dissolution shown in Fig. S2a, b), which covered the observed pH gradient and included sediments from each ecosystem. The sum of OCP and CFAP represents more soluble Ca-P (similar to $Ca\text{-}P_{meta}$) and was termed $Ca\text{-}P_{OCP+CFAP}$. Phosphate concentrations in chemical extracts were determined after Murphy and Riley (1962) using a UV–visible spectrophotometer (Cintra 2020; GBC Scientific Equipment, Dandenong, Australia).

Particle size was analysed using laser diffractometry (Mastersizer, 2000; Malvern Instruments Ltd., Malvern, UK; sediment dispersed in 10 % sodium hexametaphosphate solution). Salinity was determined by means of a TetraCon 325 electrode (WTW, Weilheim, Germany; wet sediment to deionized water ratio: 1 : 5). Nitrogen content was measured using a C / N elemental analyzer (TruSpec CNS; LECO soil 1016 for calibration; LECO Corp., St. Joseph, USA).

Concentrations of P fractions and proportions of more soluble Ca-P phases in sediments of the Firth of Thames site were compared with those of a contrasting low P site in the Saigon River delta (Oxmann et al., 2008, 2010). The site was located in the UNESCO Biosphere Reserve Can Gio close to the South China Sea and was not significantly influenced by anthropogenic P inputs. The region is not used for agriculture and the Saigon River downriver from Ho Chi Minh City (ca. 50 km from the study site) did not contain high levels of P (Schwendenmann et al., unpublished data). In contrast, the physical–chemical sediment characteristics measured at the two sites were comparable. For example, pH, Eh and salinity showed similar gradients along the land–sea transects of both sites and these parameters had similar ranges and mean values for mangrove sediments of both sites (Sect. 3.4). An area of acid sulfate sediments at the low P site was analysed separately and confirmed results of the site comparison despite its significantly lower pH values (Sect. 3.4).

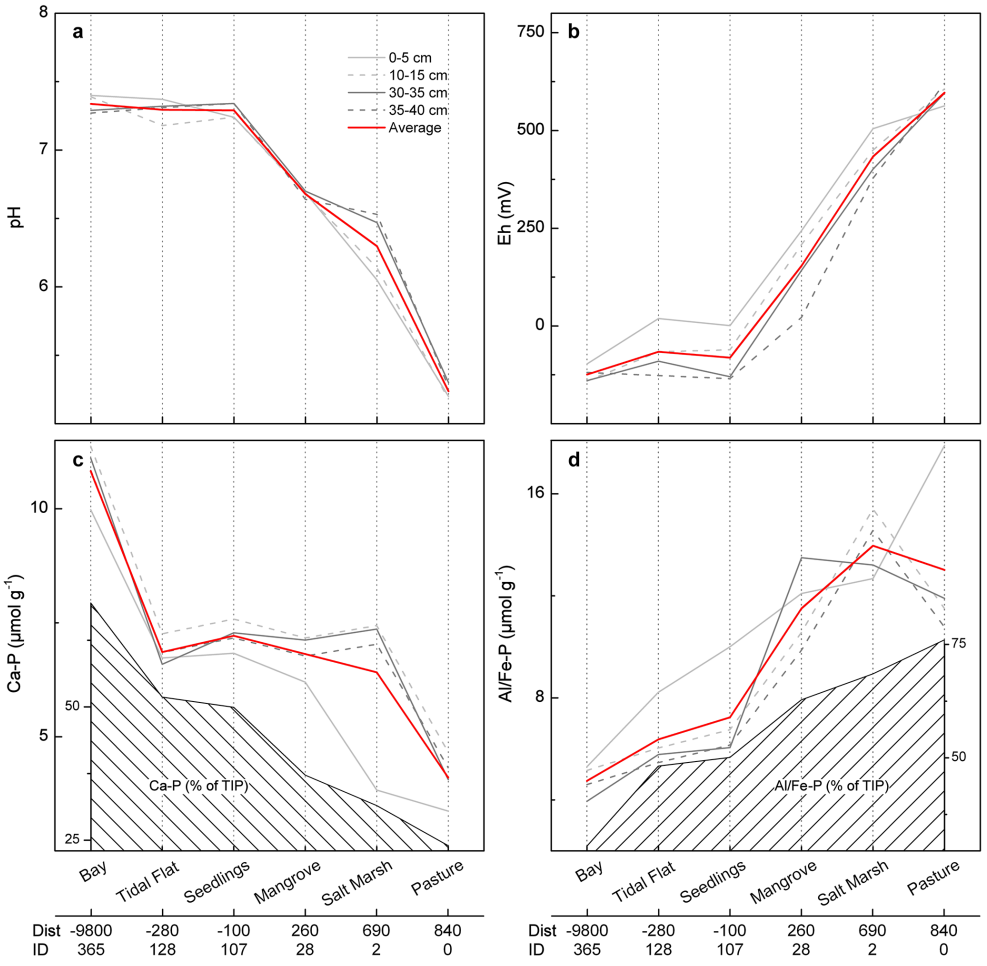

Figure 2. Physical–chemical sediment characteristics – **(a)**: pH; **(b)**: Eh – and sediment phosphorus fractions – **(c)**: Ca-P; **(d)**: Al / Fe-P – across ecosystems at the Firth of Thames. Each depth interval includes average values of several plots of each ecosystem across the entire site (all transects; see Table S1 for the number of averaged data and their values). Mean values of all depth intervals (112 samples) are also shown for each parameter. Mean fraction concentrations in % of total inorganic P (TIP) are given in **(c)** and **(d)**; x axis labels include mean distance (Dist, metres, mangrove seaward margin is set as zero) and mean inundation durations (ID; days yr^{-1}); r and p values for correlations among these parameters are given in Table 1.

3 Results

3.1 Particle size, pH and Eh

Inundation duration ranged from 365 days yr^{-1} in the bay to 0 days yr^{-1} in the pastures (Supplement Table S1). Clay, silt and sand fractions varied between 0 and 20, 60 and 80 and 0 and 30 %, respectively (not shown). Particle size distribution differed only slightly among transects. In contrast, considerable differences in particle size distribution were found along transects with higher silt and lower sand contents in mangrove plots. Salinity decreased from the bay (32 ‰) to tidal flats (21 ‰). The highest values were measured in the mangroves (35 ‰), which declined to 25 ‰ in the salt marshes and 0 ‰ in the pastures (Table S1). Sediment water content ranged between 60 and 70 % in the bay, tidal flat and mangrove fringe plots and decreased to 20–30 % in the pastures (not shown).

Sediment pH ranged from 5.18 in the pastures to 7.4 in the bay (Fig. 2a, b; Table S1). Redox potential varied between 621 mV in the pastures and −141 mV in the bay (Fig. 2a, b; Table S1). This pronounced and relatively constant pH increase and Eh decrease towards the bay was closely correlated with inundation duration (Fig. 2a, b; $p < 0.0001$). While systematic differences among depth intervals were less apparent for pH, Eh typically decreased with increasing sediment depth (Fig. 2b).

3.2 Phosphorus fractions: transformations

Ecosystem-averaged Ca-P concentrations varied considerably and ranged from 3.37 µmol g^{-1} (pastures, 0–5 cm)

Table 1. Correlations between physical–chemical sediment characteristics and P fractions at P-enriched transects of the Firth of Thames, New Zealand.

Correlation			n	Subset[a]	r	p[b]
pH	vs.	Eh	112		−0.83561	2.2×10^{-30}
Ca-P	vs.	pH	112		0.60525	1.6×10^{-12}
Ca-P	vs.	$Ca\text{-}P_{meta}$	112		0.57074	5.0×10^{-11}
Al/Fe-P	vs.	Eh	112		0.54742	4.2×10^{-10}
Al/Fe-P	vs.	pH	28	0–5 cm	−0.81043	1.7×10^{-07}[c]
$Ca\text{-}P_{meta}$	vs.	pH	112		0.44885	6.9×10^{-07}
Al/Fe-P	vs.	pH	112		−0.43497	1.6×10^{-06}[c]
Al/Fe-P	vs.	Eh	77	pH > 6.6	0.50890	2.3×10^{-06}
Al/Fe-P	vs.	Eh	28	Surface	0.75979	2.7×10^{-06}
Al/Fe-P	vs.	pH	77	pH > 6.6	−0.48749	6.9×10^{-06}
Ca-P	vs.	Salinity	112		0.39824	1.4×10^{-05}
$Ca\text{-}P_{meta}$	vs.	Eh	112		−0.26717	4.4×10^{-03}
Ca-P	vs.	Al/Fe-P	112		−0.26236	5.2×10^{-03}[d]
Al/Fe-P	vs.	Eh	35	pH < 6.6	0.15496	NS
Al/Fe-P	vs.	$Ca\text{-}P_{meta}$	112		0.09103	NS
Al/Fe-P	vs.	Salinity	112		−0.13359	NS

Al/Fe-P: Al/Fe-bound P; Ca-P: calcium-bound P; $Ca\text{-}P_{meta}$: metastable Ca-P. [a] Blank rows indicate complete sample set analysed. [b] All correlations with organic P non-significant. [c] Surface layer showed a stronger correlation between Al / Fe-P and pH than the complete data set because other depth intervals showed a peak at pH 6.6 (see Fig. 3c). [d] Note that r and p values of Ca-P vs. Al / Fe-P strongly depend on selected pH intervals (cf. Fig. 3c). NS: non-significant

Table 2. Phosphorus fractions at different pH intervals in sediments of the high P site (Firth of Thames) and low P site (Saigon River delta).[a]

Site	n		pH		Ca-P µmol g^{-1}		Al / Fe-P µmol g^{-1}	
	< 6.6	> 6.6	< 6.6	> 6.6	< 6.6	> 6.6	< 6.6	> 6.6
High P	35	72	5.9	7.0	5.92	7.69	13.65	8.90
Low P	66	23	6.0	6.9	3.55	4.10	8.03	7.89
% Increase					+49	**+ 88**	**+ 70**	+13

Ca-P: calcium-bound P (mean); Al / Fe-P: Al / Fe-bound P (mean). [a] The analysis was restricted to sediments at overlapping pH intervals for both sites (pH < 6.6: 4.83–5.99; pH > 6.6: 6.01–7.47) to compare the increase for similar mean pH values at the lower (average pH ∼ 6) and upper (average pH ∼ 7) pH intervals. Note the pH-dependent accumulation of Al / Fe-P and Ca-P (bold; Sect. 4.4).

to 11.37 µmol g^{-1} (bay, 10–15 cm) (Fig. 2c, d; Table S1). In contrast, Al / Fe-P was highest in the pastures (17.9 µmol g^{-1}; 0–5 cm) and lowest in the bay (3.94 µmol g^{-1}; 30–35 cm). On average, the lowest Ca-P and the highest Al / Fe-P concentrations were measured in 0–5 cm depth (Fig. 2c, d). Averaged percentages of Ca-P (% of TIP) steadily increased and averaged percentages Al / Fe-P (% of TIP) steadily decreased from pastures to bay (Fig. 2c, d). Along the marked downstream transition from Al / Fe-P (2.7-fold decrease) to Ca-P (2.6-fold increase), the average drop in Al / Fe-P from pastures to bay approximately matched the average Ca-P increase (−8.27 vs. +6.73 µmol g^{-1}; averages across all plots and depth intervals of each ecosystem; Table S1). Furthermore, mean Al / Fe-P concentrations in the different systems were negatively correlated with those of Ca-P ($r = -0.66$, $p < 0.001$; Table S1). In addition, the decline in Al / Fe-P with depth was counterbalanced by the Ca-P increase with depth (−1.16 vs. +1.18 µmol g^{-1}; Table S1). Pastures were excluded from estimating these changes with depth because here the large loss of Al / Fe-P with depth was not counterbalanced by Ca-P (apparent surface runoff: −6.00 vs. +0.69 µmol g^{-1}; Table S1).

3.3 Phosphorus fractions: P load, pH and Eh effects

Mean sediment Ca-P concentration at the high P site was approximately twice the level of Ca-P at the low P site (Fig. 3a). Mean sediment Al / Fe-P concentration was approximately 30 % higher at the high P site compared to the low P site. However, at both sites Ca-P increased strongly with pH (Fig. 3a). Al / Fe-P showed a peak at ∼ pH 6.6

Table 3. Phosphorus fractions in mangrove sediments of the high P site (Firth of Thames) and low P site (Saigon River delta).

Mangrove site	n	pH	Eh mV	Ca-P µmol g^{-1}	Al / Fe-P µmol g^{-1}	Ca-P_{meta} µmol g^{-1}	Ca-P_{meta} (% of Ca-P)
High P	48	6.8	95	6.91	10.44	2.35	34
Low P	64	6.4	66	3.85	8.36	0.40	10
Low P_{acid} [a]	(32)	(5.0)	(240)	(2.78)	(6.26)	(0.27)	(10)
% Increase [b]				**+80** (+150)	**+25** (+65)	**+482** (+800)	**+240** (+240)

Ca-P: calcium-bound P (mean); Al / Fe-P: Al / Fe-bound P (mean); Ca-P_{meta}: metastable Ca-P (mean). [a] Area of acid sulfate sediments in mangroves of the low P site. [b] Percentages of P fraction increase at the high P site in comparison to the low P site (bold), which had similar pH and Eh values. Values for a comparison of the high P site with an area of acid sulfate sediments (Low P_{acid}) in parentheses.

Table 4. Correlation coefficients (for $p < 0.05$) between concentrations of P fractions, OCP, CFAP, FAP and pH in sediments analysed for particular Ca-P species.[a]

	Al / Fe-P	Res. P	pH	FAP	CFAP	OCP	Ca-P	OCP+CFAP	Ca-P_{meta}
Res. P	0.88****								
pH	[b]	–							
FAP	–	–	–						
CFAP	–	0.69**	–	–					
OCP	–	–	–	–	–				
Ca-P	[b]	–	0.68*	–	0.77**	0.81***			
OCP+CFAP	–	–	0.88****	–	0.65*	0.67*	0.79**		
Ca-P_{meta}	–	–	–	–	0.84**[c]	–	0.76*[c]	0.74*[c]	
TIP	0.95****	0.91****	–	–	0.66*	–	–	–	0.69*[c]

TIP: total inorganic P; Al / Fe-P: Al / Fe-bound P; Ca-P: calcium-bound P; Ca-P_{meta}: metastable Ca-P; OCP: octacalcium phosphate; CFAP: carbonate fluorapatite; FAP: fluorapatite; Res. P: residual P. NS is non-significant; * is 0.05 level; ** is 0.01 level; *** is 0.001 level; **** is 0.0001 level. [a] Species distributions shown in Fig. 5. [b] See Fig. 3 for correlations among Ca-P, Al / Fe-P and pH using a larger set of fraction data. [c] $n = 9$; for all other correlations $n = 13$.

(Fig. 3b). Thus, despite large differences in P fraction concentrations between the two sites pH dependencies of both fractions were similar, except for Al / Fe-P concentrations in 0–5 cm depth. Concentrations of Al / Fe-P in this depth range showed a continuous decrease with pH at the high P site due to high Al / Fe-P levels in acidic surface sediment of the pastures (linear regression in Fig. 3b; Table 1; $r = -0.81$, $p < 0.0001$).

In sediments with pH < 6.6 the average concentration of Al / Fe-P was 70 % higher at the high P site than at the low P site (Table 2; Fig. 3b). Despite these largely elevated levels of Al / Fe-P at topographically higher areas, Al / Fe-P was only slightly increased (13 %) in the lower intertidal zones and the bay (pH > 6.6; Table 2; Fig. 3b). Calcium phosphate in contrast showed the opposite pattern of enrichment at the high P site. In comparison to the low P site the average concentration of Ca-P was only 49 % higher in the upper intertidal zones and pastures (pH < 6.6) but increased by 88 % in the lower intertidal zones and the bay (pH > 6.6; Table 2; Fig. 3a).

Although Ca-P and Al / Fe-P clearly showed opposite trends along the three transects of the high P site (Fig. 2c, d), both fractions increased strongly with pH below pH 6.6 (Fig. 3a, b). Both fractions were positively correlated at pH < 6.6 (shown in Fig. 3c for lower depth of both sites). At pH > 6.6, however, Ca-P increased further, whereas Al / Fe-P abruptly decreased (cf. Fig. 3a and b). Because this switch occurred in the landward to seaward direction, it is in agreement with the observed Ca-P increase and Al / Fe-P decrease towards the bay (Fig. 2c, d).

3.4 Metastable calcium phosphate

Metastable Ca-P (Ca-P_{meta}) increased strongly with pH (Fig. 4a; Firth of Thames cross-data-set correlations in Table 1), similar to Ca-P (Fig. 3a), and correlated with Ca-P at both sites (Fig. 4b; Table 1). Yet sediments of the high P site contained on average 6-fold higher concentrations of Ca-P_{meta} compared with the low P site (Fig. 4c). In contrast, sediments of the high P site contained only 2-fold more total Ca-P than those of the low P site (Fig. 3a). On average, Ca-P_{meta} comprised ca. 35 % of total Ca-P at the high P site and only 10 % at the low P site (Fig. 4d).

To verify that the higher Ca-P_{meta} concentrations were not a consequence of site-specific differences in vegetation or physical–chemical sediment conditions we restricted the comparison to mangrove plots, which showed similar ranges and mean values of pH, Eh and salinity at both sites (Firth of

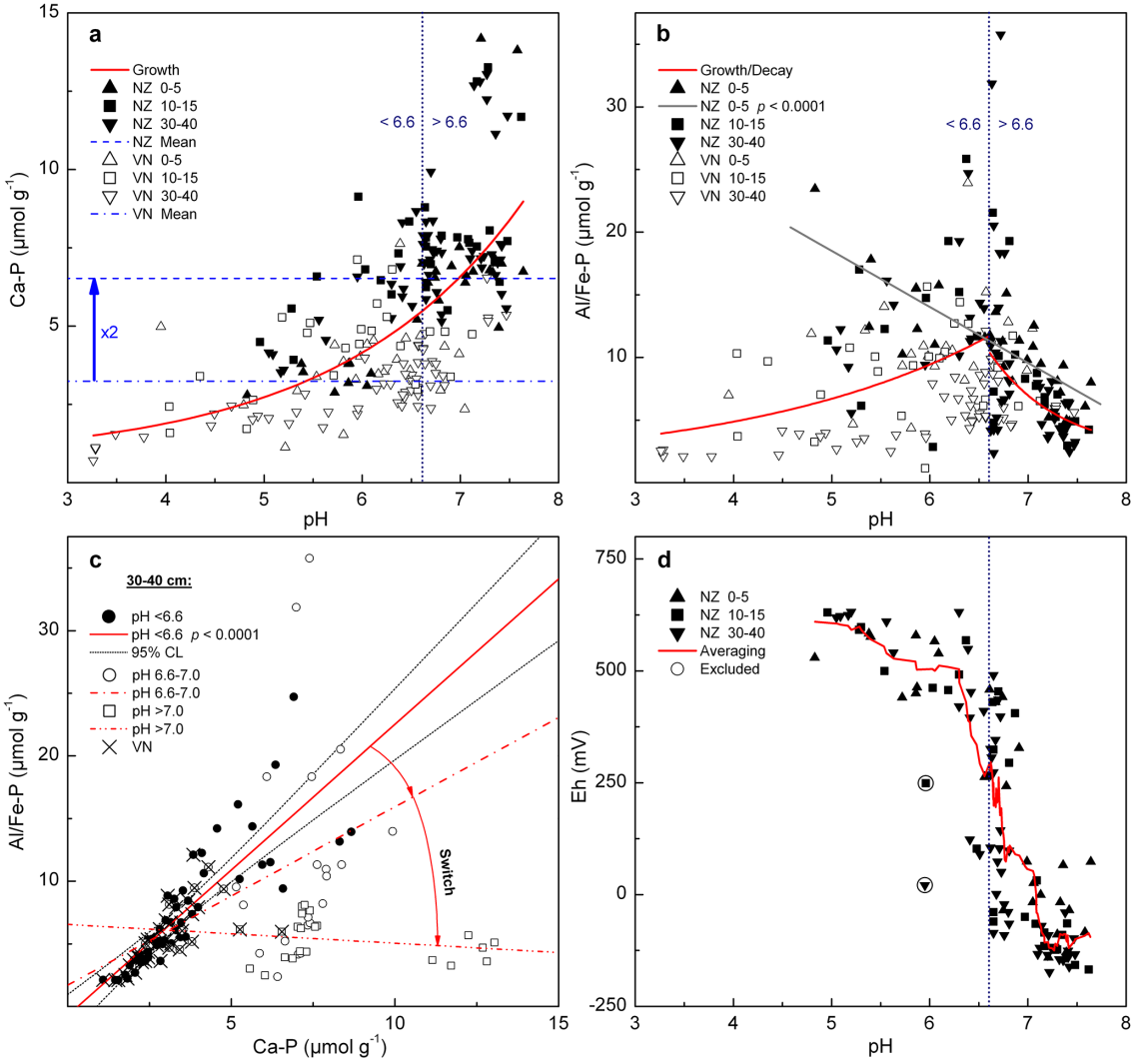

Figure 3. Changes of sediment phosphorus fractions (Al / Fe-P; Ca-P) as a function of pH and Eh variations at transects at the Firth of Thames (NZ) and Saigon River delta (VN) site. **(a)** Ca-P increase with pH (exponential; both sites, all samples). Mean Ca-P concentration of Firth of Thames samples ca. twice that of Saigon River delta samples. **(b)** Al / Fe-P peak at ~ pH 6.6 due to increase below and decrease above that value (exponential; both sites, all samples). **(c)** Linear regressions between Al / Fe-P and Ca-P at deeper depths (30–35, 35–40 cm) for different pH intervals (cf. Fig. 3a, b). Arrows indicate switch from Al / Fe-P to Ca-P with increasing pH (seaward direction). **(d)** Eh vs. pH (NZ; all samples). Different symbols denote surface (0–5 cm), intermediate (10–15 cm) and deeper depth intervals (30–35, 35–40 cm) in **(a)**, **(b)** and **(d)**. Symbols for VN data marked with cross in **(c)**. Smoothing by averaging 10 adjacent Eh values of pH sorted data in **(d)**. See text for linear regression in **(b)**.

Thames: pH 5.8–7.1, −160–450 mV, 25–50 ‰; Saigon River delta: pH 5.7–7.0, −180–400 mV; 25–40 ‰; Table 3). This adjustment did not change the results. The difference in Ca-P_{meta} concentrations between mangrove plots of the two sites was just as disproportionate when compared to the difference in total Ca-P concentrations between those plots (6-fold vs. 2-fold). The portion of Ca-P_{meta} was still ca. 35 % at the high P site and 10 % at the low P site (Table 3). Moreover, the proportion of Ca-P_{meta} to total Ca-P was equally low for an area of acid sulfate sediments of the low P site (10 %) despite its very different average pH and Eh values (Table 3). In summary, comparatively large amounts of metastable Ca-P accumulated at the high P site.

3.5 Octacalcium phosphate and authigenic apatite

Distributions of OCP, authigenic apatite and detrital apatite were related to the pH at both sites. Strongly acidic sediments (~ pH < 4) contained just detrital apatite (FAP), whereas slightly acidic sediments (~ pH 4–7) contained also authigenic apatite (CFAP). Octacalcium phosphate was additionally present in alkaline mangrove, river, bay and tidal flat

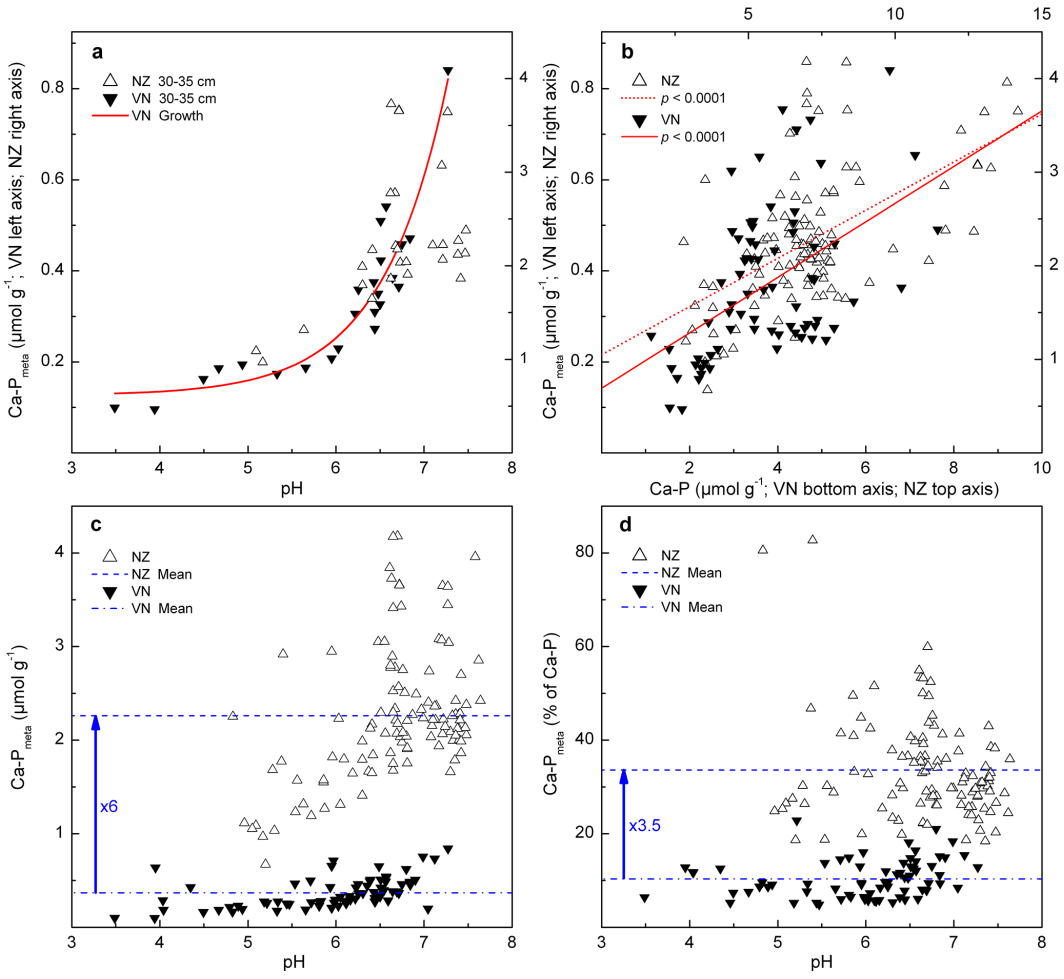

Figure 4. Accumulation and pH dependence of metastable Ca-P (Ca-P_{meta}) along transects at the Firth of Thames (NZ) site compared to the Saigon River delta (VN) site. **(a)** Increase of Ca-P_{meta} with pH (exponential; 30–35 cm). **(b)** Linear regressions of Ca-P_{meta} vs. total Ca-P (all plots and depths; NZ: $r = 0.57$, $p < 0.0001$; VN: $r = 0.50$, $p < 0.0001$). **(c)** Ca-P_{meta} vs. pH (all plots and depths). Mean Ca-P_{meta} concentration at the Firth of Thames site ca. 6 times that of the Saigon River delta site. **(d)** Ca-P_{meta} in % of total Ca-P vs. pH (all plots and depths). Mean percentage ca. 3.5 times higher for the Firth of Thames site. Note different axis ranges for the two sites in **(a)** and **(b)**.

sediments. Hence, the concentration of more soluble Ca-$P_{OCP+CFAP}$ (hatched area in Fig. 5) significantly increased with pH ($r = 0.88$, $p < 0.0001$; Table 4). However, the portion of Ca-$P_{OCP+CFAP}$ as a percentage of total Ca-P was significantly larger (70.5 ± 17.5 %; numbers above columns in Fig. 5) for sediments of the high P site compared to the low P site (29.5 ± 26.0 %, $t(11) = 3.346$, $p = 0.0065$). This larger portion of Ca-$P_{OCP+CFAP}$ provided supporting evidence for the larger portion of Ca-P_{meta} in sediments of the high P site (cf. Sect. 3.4). Overall, more soluble Ca-P determined by the two independent methods (CONVEX method: Ca-$P_{OCP+CFAP}$; Morgan test: Ca-P_{meta}) yielded comparable results. Accordingly, corresponding values obtained by the two methods were significantly correlated ($r = 0.74$, $p < 0.05$; Table 4).

4 Discussion

4.1 Phosphorus status, Firth of Thames

The Firth of Thames sediments were high in P compared to the Saigon River delta site and sediments from other coastal areas (Tables 3 and S3; Figs. 3, 4). Total P concentrations measured along the three transects are classified as enriched (> 16 µmol P g^{-1}) and very enriched (> 32 µmol P g^{-1}) according to the New Zealand classification system (Robertson and Stevens, 2009; Sorensen and Milne, 2009). This is due largely to high P fertilizer application rates, which constitute the main P source (~ 90 %) to the watershed (Waikato region; total input: 41 Gg P yr^{-1}; fertilizer: 37 Gg P yr^{-1}; rate: 28 kg P ha^{-1} yr^{-1}; atmosphere and weathering: 4 Gg P yr^{-1}; Parfitt et al., 2008). A significant increase in TP is correlated with intensification of pastoral farming and contributes to

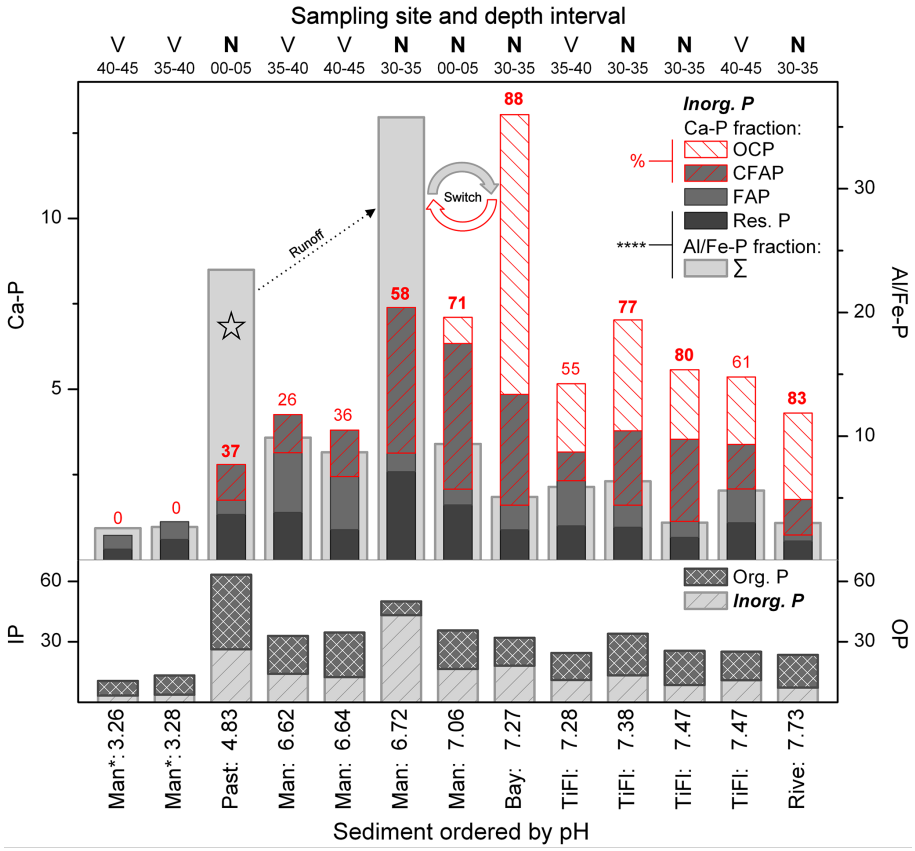

Figure 5. Phosphorus species distributions in sediments of different ecosystems at the Firth of Thames (NZ) and Saigon River delta (VN), ordered by pH (all concentrations in µmol P g^{-1}). The top axis shows the sampling site (N: NZ, New Zealand; V: VN, Vietnam) and depth interval (cm). The portion of more soluble Ca-$P_{OCP+CFAP}$ (hatched area) is given as a percentage of total Ca-P above columns (NZ values in bold). A typical decrease of adsorbed P and increase of OCP with increasing pH from 6.7 to 7.3 suggests a reversible transformation in that range (arrows; adsorption–precipitation switch). Strong Al / Fe-P predominance in acidic surface sediment of the pasture is denoted (star). Org. P: total organic P; Inorg. P: total inorganic P; OCP: octacalcium phosphate; CFAP: carbonate fluorapatite; FAP: fluorapatite; Res. P: residual P; Man*: strongly acidic mangrove; Man: mangrove; Past: pasture; TiFl: tidal flat; Rive: river. Residual P correlated with Al / Fe-P at a significance level of 0.0001 (asterisks). See Table 4 for all correlations among species distributions.

the deterioration of the river water quality by surface runoff (Vant and Smith, 2004). Further, elevated levels of P and nitrogen in groundwater at coastal farmlands agreed with specific fertilizer application rates (Brownell, 2004). The application rates and previous findings strongly suggest that the P accumulation measured in this study was largely related to P fertilization practices. Hence, the Firth of Thames site is characterized by anthropogenic P enrichment.

4.2 Phosphorus fractions

Phosphorus fractions showed a strong and continuous increase of Ca-P and decrease of Al / Fe-P with increasing inundation duration (Fig. 2). These changes were driven by pH and Eh gradients (Fig. 2). Salinity had no detectable effect on Al / Fe-P (Table 1), similar to findings of Maher and DeVries (1994). Both an increase in Ca-P (decreasing solubility of calcium phosphates with increasing pH; Lindsay et al., 1989; Hinsinger, 2001) and a decline in Al / Fe-P (desorption of P from metal (hydr)oxides with increasing pH or decreasing Eh; e.g. Mortimer, 1971) commonly occur across estuarine inundation gradients. A similar seaward redistribution of sediment P fractions has been observed, for example, in marsh systems in Portugal (Coelho et al., 2004) and South Carolina (Paludan and Morris, 1999), estuarine zones of a French river (Andrieux-Loyer et al., 2008) and an estuarine transect from the Mississippi River to the Gulf of Mexico (Sutula et al., 2004). In the latter case, the opposing landward-to-seaward changes in sediments (Sutula et al., 2004) were mirrored by similar changes in corresponding samples of surface water particulate matter. Furthermore, the same trends were observed along a continuum from agricultural soils across hard-water stream sediments to lake sediments (Noll et al., 2009).

The pH dependence of the solubility of Ca-P phases was mirrored by the increase in Ca-P with decreasing acidity

(Fig. 3a). In contrast, concentrations of Al / Fe-P showed a maximum amount of adsorbed P at pH 6.6 (Fig. 3b) and therefore agreed with the commonly occurring maximum P availability at pH 6.5 in agricultural soils (e.g. Chapin III et al., 2011). This maximum P availability is caused by the highest P solubility in equilibrium with various P minerals at pH 6.5 (Lindsay et al., 1989). Considering that low amounts of P are precipitated with Ca, Fe and Al at pH 6.5 (e.g. Chapin III et al., 2011), large amounts of soluble reactive P could be available for adsorption on metal (hydr)oxides. Further, Ca-P phases predominated in alkaline downstream environments and may undergo dissolution after upstream transport by tides with an accompanying increase in P adsorption (cf. Fig. 2a, c, d; De Jonge and Villerius; 1989). If these phases are transported to close locations of ∼ pH 6.5 and subsequently dissolve, the phosphate released can be adsorbed on more oxidized sediment, thereby contributing to the elevated Al / Fe-P concentrations at this pH.

The maximum amount of adsorbed P at pH 6.6 also indicated that Eh, which showed the maximum decline at ∼ pH 6.6 (Fig. 3d), did not cause significant desorption of P at this pH. Below this pH, Al / Fe-P did not decline with Eh (cf. Fig. 3b and d) and these parameters were not correlated (Table 1), suggesting that a release of P adsorbed to ferric iron compounds did not occur in the corresponding sediments. Yet, both Eh and Al / Fe-P decreased above pH 6.6 (cf. Fig. 3b and d) and were correlated in this range (Table 1). Because the drop in Al / Fe-P correlated also with an increase in pH (Table 1, Fig. 3b), effects of pH and Eh on P desorption could not be distinguished above pH 6.6. The decreasing amount of adsorbed P at near-neutral to alkaline pH may therefore be due to (i) charge changes of metal (hydr)oxides with pH (Oh et al., 1999; Spiteri et al., 2008; Barrow et al., 1980; Sundareshwar and Morris, 1999), (ii) less efficient sorption by iron in the Fe(II) state compared to the Fe(III) state (e.g. Sundareshwar and Morris, 1999), or (iii) a combination of charge changes and Fe reduction.

Critical redox potentials reported for reduction of ferric iron compounds are around 300 mV at pH 5 and 100 mV at pH 7 (Gotoh and Patrick, 1974; Husson, 2013; Yu et al., 2007). These levels match very well with critical Eh levels for desorption of Fe-(hydr)oxide-bound P, including a similar pH dependence of those levels (compare Delaune et al., 1981 with Gotoh and Patrick, 1974). As Fig. 3d shows, Eh values that did not correlate with Al / Fe-P (sediments with pH < 6.6) were above the critical Eh threshold, whereas Eh values that correlated with Al / Fe-P (sediments with pH > 6.6) were below the critical Eh threshold. This implies that reductive dissolution and related desorption of P could have contributed to the downstream transition from Al / Fe-P to Ca-P. Interestingly, the physicochemically induced P redistribution largely agreed with that from the low P site despite considerable differences of P fraction concentrations between both sites (Fig. 3a, b). This suggests that the effects of physical–chemical sediment characteristics were independent of the site-specific total P status.

4.3 Transformation of phosphorus fractions

The increase in Ca-P along transects, which correlated with an equivalent decrease in Al / Fe-P, strongly suggests that Ca-P formed at the expense of adsorbed P along the salinity gradient. By plotting Al / Fe-P and Ca-P concentrations on a pH scale (Fig. 3a, b) it became evident that the downstream transition from Al / Fe-P to Ca-P was related to a pronounced switch from P adsorption to Ca-P precipitation at ∼ pH 6.6 (see also Fig. 3c). Above this pH, reduction processes are less important for P desorption (Reddy and DeLaune, 2008), P adsorption is usually less pronounced (Murrmann and Peech, 1969) and thermodynamically less stable Ca-P phases such as OCP may form (Bell and Black, 1970; Oxmann and Schwendenmann, 2014).

A similar switch has been suggested for observed fraction changes with increasing sediment depth in non-upwelling continental margin environments, but from organic P to authigenic Ca-P (Ruttenberg and Berner, 1993). This switch was partly explained by the redox state, which could be the controlling parameter for diagenetic redistribution and related downcore changes of P fractions in marine environments. The main difference between the P redistribution in this study and results of Ruttenberg and Berner (1993) relates to the P source to the formation of authigenic Ca-P. Our results show strong interactions between inorganic P forms, with Al / Fe-P being a significant P source for Ca-P. In contrast to these strong interactions between Al / Fe-P and Ca-P all correlations with organic P were not significant.

However, the P redistribution along marine sediment cores may strongly differ from that across intertidal zones. The marked fraction changes suggest that the pH regulates an alternative switch between Al / Fe-P and Ca-P at the coastal sites investigated here. This pH-driven P redistribution could be a common mechanism at coastal pH gradients because it took place along different transects, comprising diverse ecosystems, and it was independent of the site-specific total P status (Fig. 3a, b). Hence, this mechanism could also be important for processes of P accumulation by increased P loads, as discussed next.

4.4 Phosphorus accumulation processes

The anthropogenic P input at the high P site caused two different location-dependent accumulation mechanisms, which mainly resulted in elevated Al / Fe-P at pH < 6.6 (landward) and elevated Ca-P at pH > 6.6 (seaward). The between-site comparison (high vs. low P site) therefore implies that fertilizer-derived P was largely included in the Al / Fe-P fraction (adsorbed P) of acidic landward sediments. Phosphorus inputs by runoff or erosion to downstream areas apparently led to enhanced precipitation of Ca-P by increasing pH.

The accumulation pattern in this site comparison therefore corresponds to location-dependent transformations between Al / Fe-P and Ca-P, which are to be expected from the P redistribution at individual sites (Sect. 4.3).

We hypothesize that more soluble Ca-P minerals accumulate relative to total Ca-P due to anthropogenic P inputs because the formation of sparingly soluble Ca-P minerals is too slow for balancing increased formation rates of thermodynamically less stable Ca-P minerals. This hypothesis is consistent with comparatively large amounts of metastable Ca-P, which apparently accumulated at the high P site due to external factors (Sect. 3.4, Table 3; Fig. 4c, d). Our findings showed that Morgan's weakly acidic acetate–acetic acid solution preferentially extracts metastable Ca-P phases. Because sparingly soluble Ca-P minerals, such as detrital apatite, are unlikely to dissolve in Morgan's solution (pH 4.8; cf. Ruttenberg, 1992), the correlations between Morgan P ($Ca\text{-}P_{meta}$) and Ca-P ($p < 0.0001$ at both sites; Fig. 4b) are attributable to more soluble Ca-P minerals. This conclusion is supported by other studies which have indicated that the Morgan test preferentially extracts more soluble Ca-P phases, whereas most other available P tests preferentially extract adsorbed P (cf. Ahmad et al., 1968; Curran, 1984; Curran and Ballard, 1984; Dabin, 1980; Herlihy and McCarthy, 2006).

Our hypothesis is also consistent with concentrations of OCP, CFAP and FAP, which were separately determined for sediments of both sites (Fig. 5). Sediments of the high P site showed a significantly larger portion of $Ca\text{-}P_{OCP+CFAP}$ compared to the low P site. Results of both independent methods, which were significantly correlated (Table 4), therefore provide strong evidence for the proposed accumulation of thermodynamically less stable Ca-P by anthropogenic P inputs. Less stable Ca-P may thus be a useful parameter to monitor anthropogenic accumulations of inorganic P in coastal regions. Because physical–chemical sediment characteristics influence Ca-P formation, an important caveat is the between-site comparability of data. In this study, there was between-site comparability of both the sediment characteristics and the general response of each of the P fractions and P species to the sediment characteristics at different depth intervals along the land–sea continuum (Figs. 3a, b, 4a, b, 5).

A dominant proportion of more soluble Ca-P was contributed by OCP in alkaline sediments (Fig. 5). These OCP concentrations therefore suggest authigenic apatite formation by initial precipitation of OCP in alkaline mangrove, river, bay and tidal flat sediments. Octacalcium phosphate was detected in surface marine sediment using XANES (Oxmann, 2014; XANES spectra of Brandes et al., 2007), which requires minimal sample preparation and is minimally affected by common sample matrices. Results of the CONVEX method, which was validated by the matrix effect-free method of standard addition (Oxmann and Schwendenmann, 2014), therefore agree with field and experimental evidence for the occurrence of OCP in sediment (see also Gunnars et al., 2004; Jahnke et al., 1983; Krajewski et al., 1994; Morse and Casey, 1988; Nancollas et al., 1989; Schenau et al., 2000; van Cappellen and Berner, 1988).

We conclude that OCP plays a crucial role in the redistribution of sediment P (see arrows in Fig. 5), including the pH-dependent switch from adsorbed P to Ca-P in the landward to seaward direction, the potential reverse transformation after upstream transport, and the pH-dependent accumulation processes. Further, apatite formation by successive crystallization is possibly mainly restricted to alkaline sediments. Octacalcium phosphate is an important intermediate in the formation of apatite in alkaline environments, including calcareous soil (Alt et al., 2013; Beauchemin et al., 2003; Grossl and Inskeep, 1992), lake sediment (e.g. Avnimelech, 1983) and marine sediment (see above references). In agreement with the high OCP concentrations found in this study (Fig. 5), solid-state nuclear magnetic resonance (NMR) and XANES spectroscopy-based studies implied that OCP does belong not only to the most commonly reported but also to the most prevalent inorganic P forms in alkaline environments (Beauchemin et al., 2003; Kizewski et al., 2011; Oxmann, 2014).

In general, the established Ca-P precipitation in sediments across salinity gradients provides some insight into the relevance of factors influencing this precipitation such as changes in salinity, dissolved phosphate and pH. In fact, as the ionic strength increases with increasing salinity for a given phosphate concentration and pH, the apparent Ca-P solubility increases strongly (cf. Atlas, 1975). Yet, increasing Ca-P concentrations imply that the salt effect is usually more than offset by the rise in pH, redox-driven phosphate desorption from iron oxyhydroxides and other potential factors in interstitial waters across salinity gradients. For example, Ca^{2+} concentrations generally increase from land to sea and, hence, increase the saturation state with respect to calcium phosphates (normal seawater and sediment pore water: ca. 10 mM; river water, global average: ca. 0.4 mM; soil pore water, average of temperate region soils: ca. 1.5 mM; Girard, 2004; Lerman and Wu, 2008; Lower et al., 1999; Rengel, 2006; Sun and Turchyn, 2014). Although the correlation of salinity with Al / Fe-P was not significant, the correlation with Ca-P was decreased but still significant (Table 1), indicating that increasing Ca^{2+} concentrations from land to sea may also contribute to Ca-P formation.

Our results imply that when P enters the marine environment, enhanced Ca-P formation takes place in nearshore environments. Given the possibility that CFAP or other less stable Ca-P phases do not readily dissolve in alkaline seawater (Faul et al., 2005; Lyons et al., 2011; Sheldon, 1981; see also Gulbrandsen et al., 1984 as cited in Slomp, 2011), some non-detrital Ca-P at sites further offshore could be derived from Ca-P-generating areas of the lower intertidal zone or even from freshwater environments (see e.g. Raimonet et al., 2013).

5 Conclusions

Our results show a pH-induced switch from P adsorption to Ca-P precipitation at near-neutral pH, which apparently leads to inorganic P accumulation in nearshore sediments. The decrease in Eh and increase in Ca^{2+} concentrations from land to the sea likely contribute to this switch. Further, this P redistribution is apparently driven by OCP formation and enhanced by anthropogenic P inputs. Hence, a significant proportion of authigenic Ca-P may be derived from anthropogenic sources in some coastal regions.

The proposed mechanism, including relatively rapid formation of an apatite precursor, explains several independent observations: the downstream transition from Al / Fe-P to Ca-P at ∼ pH 6.6, the Ca-P formation at the expense of adsorbed P, the large increase of $Ca\text{-}P_{meta}$ with increasing pH, the dominant proportion of OCP in alkaline sediments, the pH-dependent accumulation mechanisms of Al / Fe-P and Ca-P, and the accumulation of $Ca\text{-}P_{meta}$ and $Ca\text{-}P_{OCP+CFAP}$ at the high P site. The suggested switch appears to be a very common mechanism because it was observed across different ecosystems and it was independent of the site-specific total P status. Further evidence that this mechanism operates in different environments comes from similar downstream transitions reported by several studies.

Less stable Ca-P is mainly formed and buried during sedimentation rather than being allochthonous material. Hence, CFAP and OCP act as diagenetic sinks for P at the investigated sites and are mainly responsible for the accumulation of inorganic P in the lower intertidal zone and bay. Some authigenic Ca-P, however, could be dissolved when physical–chemical conditions of the sediment change (e.g. altered pH/Eh due to land reclamation) or after upstream transport by tides. Some of it could also be resuspended and transported further offshore, similar to detrital FAP. In general, OCP formation may mitigate a desorption-derived P release from sediment and seems to occur when P adsorption is usually less pronounced – that is, under alkaline conditions.

The Supplement related to this article is available online at doi:10.5194/bg-12-723-2015-supplement.

Acknowledgements. We thank Bharath Thakur for assistance in field work and sample preparation and Peter and Gail Thorburn for assistance with sampling by boat. The project was funded by the German Research Foundation through a research fellowship granted to J. F. Oxmann under the code OX 54/2-1.

The service charges for this open-access publication have been covered by a Research Centre of the Helmholtz Association.

Edited by: C. P. Slomp

References

Ahmad, N., Jones, R. L., and Beavers, A. H.: Genesis, mineralogy and related properties of West Indian soils, (i) Montserrat Series, derived from glauconitic sandstone, Central Trinidad, J. Soil Sci., 19, 1-8, 1968.

Alt, F., Oelmann, Y., Schöning, I., and Wilcke, W.: Phosphate release kinetics in calcareous grassland and forest soils in response to H^+ addition, Soil Sci. Soc. Am. J., 77, 2060–2070, 2013.

Andersen, J. M.: An ignition method for determination of total phosphorus in lake sediments, Water Res., 10, 329–331, 1976.

Andrieux-Loyer, F., Philippon, X., Bally, G., Kéroul, R., Youenou, A., and Le Grand, J.: Phosphorus dynamics and bioavailability in sediments of the Penzé Estuary (NW France): in relation to annual P-fluxes and occurrences of *Alexandrium Minutum*, Biogeochemistry, 88, 213–231, 2008.

Anjos, J. T. and Rowell, D. L.: The effect of lime on phosphorus adsorption and barley growth in three acid soils, Plant Soil, 103, 75–82, 1987.

Atlas, E. L.: Phosphate equilibria in seawater and interstitial waters, Ph.D. thesis, Oregon State University, Corvallis, 1975.

Atlas, E. L. and Pytkowicz, R. M.: Solubility behavior of apatites in seawater, Limnol. Oceanogr., 22, 290–300, 1977.

Avnimelech, Y.: Phosphorus and calcium carbonate solubilities in Lake Kinneret, Limnol. Oceanogr., 28, 640–645, 1983.

Barrow, N. J., Bowden, J. W., Posner, A. M., and Quirk, J. P.: Describing the effects of electrolyte on adsorption of phosphate by a variable charge surface, Aust. J. Soil Res., 18, 395–404, 1980.

Baturin, G. N. (Ed.): Principal features of the marine geochemistry of disseminated phosphorus, in: Developments in Sedimentology, Elsevier B. V., Amsterdam, 1981.

Beauchemin, S., Hesterberg, D., Chou, J., Beauchemin, M., Simard, R. R., and Sayers, D. E.: Speciation of phosphorus in phosphorus-enriched agricultural soils using X-ray absorption near-edge structure spectroscopy and chemical fractionation, J. Environ. Qual., 32, 1809–1819, 2003.

Bell, L. C. and Black, C. A.: Transformation of dibasic calcium phosphate dihydrate and octacalcium phosphate in slightly acid and alkaline soils, Soil Sci. Soc. Am. Proc., 34, 583–587, 1970.

Bentor, Y. K. (Ed.): Phosphorites: The unsolved problems, in: Marine Phosphorites: Geochemistry, occurrence, genesis, SEPM Special Publication, 29, 3–18, 1980.

Bolan, N. S., Adriano, D. C., and Curtin, D.: Soil acidification and liming interactions with nutrient and heavy metal transformation and bioavailability, Adv. Agron., 78, 215–272, 2003.

Bowden, J. W., Nagarajah, S., Barrow, N. J., and Quirk, J. P.: Describing the adsorption of phosphate, citrate and selenite on a variable-charge mineral surface, Aust. J. Soil Res., 18, 49–60, 1980.

Brandes, J. A., Ingall, E., and Paterson, D.: Characterization of minerals and organic phosphorus species in marine sediments using soft X-ray fluorescence spectromicroscopy, Mar. Chem., 103, 250–265, 2007.

Brownell, B.: Firth of Thames RAMSAR Site update, EcoQuest Education Foundation, Kaiaua, New Zealand, 2004.

Chapin III, F. S., Matson, P. A., and Vitousek, P. M.: Principles of terrestrial ecosystem ecology, 2nd Edn., Springer-Verlag, New York, 529 pp., 2011.

Clarke, P. J.: Nitrogen pools and soil characteristics of a temperate estuarine wetland in eastern Australia, Aquat. Bot., 23, 275–290, 1985.

Coelho, J. P., Flindt, M. R., Jensen, H. S., Lillebø, A. I., and Pardal, M. A.: Phosphorus speciation and availability in intertidal sediments of a temperate estuary: Relation to eutrophication and annual P-fluxes, Estuar. Coast. Shelf. S., 61, 583–590, 2004.

Curran, M. P.: Soil testing for phosphorus availability to some conifers in British Columbia, B.Sc. thesis, The University of Victoria, B.C., 1984.

Curran, M. P. and Ballard, T. M.: P availability to forest trees in British Columbia, Contract Res. Rep. to B.C. Ministry of Forests, Victoria, B.C., 1984.

Dabin, P.: Phosphorus deficiency in tropical soils as a constraint on agricultural output, priorities for alleviating soil-related constraints to food production in the tropics, IRRI, Los Banos, 217–233, 1980.

De Jonge, V. N. and Villerius, L. A.: Possible role of carbonate dissolution in estuarine phosphate dynamics. Limnol. Oceanogr., 34, 332–340, 1989.

DeLaune, R. D., Reddy, C. N., and Patrick, W. H., Jr.: Effect of pH and redox potential on concentration of dissolved nutrients in an estuarine sediment, J. Environ. Qual., 10, 276–279, 1981.

Eisma, D.: Intertidal deposits: River mouths, tidal flats and coastal lagoons, CRC Press, Boca Raton, Boston, London, New York, 525 pp., 1997.

Faul, K. L., Paytan, A., and Delaney, M. L.: Phosphorus distribution in sinking oceanic particulate matter, Mar. Chem., 97, 307–333, 2005.

Fauzi, A., Skidmore, A. K., Heitkönig, I. M. A., van Gils, H., and Schlerf, M.: Eutrophication of mangroves linked to depletion of foliar and soil base cations, Environ. Monit. Assess., 186, 8487–8498, 2014.

Gao, Y., Cornwell, J. C., Stoecker, D. K., and Owens, M. S.: Effects of cyanobacterial-driven pH increases on sediment nutrient fluxes and coupled nitrification-denitrification in a shallow fresh water estuary, Biogeosciences, 9, 2697–2710, doi:10.5194/bg-9-2697-2012, 2012.

Girard, J.: Principles of environmental chemistry, Jones and Bartlett Publishers, Sudbury, Massachusetts, 2004.

Golubev, S. V., Pokrovsky, O. S., and Savenko, V. S.: Unseeded precipitation of calcium and magnesium phosphates from modified seawater solutions, J. Cryst. Growth, 205, 354–360, 1999.

Gotoh, S. and Patrick, W. H.: Transformation of iron in a waterlogged soil as influenced by redox potential and pH, Soil Sci. Soc. Am. J., 38, 66–71, 1974.

Grossl, P. R. and Inskeep, W. P.: Kinetics of octacalcium phosphate crystal growth in the presence of organic acids, Geochim. Cosmochim. Ac., 56, 1955–1961, 1992.

Gulbrandsen, R. A., Roberson, C. E., and Neil, S. T.: Time and the crystallization of apatite in seawater, Geochim. Cosmochim. Ac., 48, 213–218, 1984.

Gunnars, A., Blomqvist, S., and Martinsson, C.: Inorganic formation of apatite in brackish seawater from the Baltic Sea: an experimental approach, Mar. Chem., 91, 15–26, 2004.

Hartzell, J. L. and Jordan, T. E.: Shifts in the relative availability of phosphorus and nitrogen along salinity gradients, Biogeochemistry, 107, 489–500, 2012.

Haynes, R. J.: Effects of liming on phosphate availability in acid soils – A critical review, Plant Soil, 68, 289–308, 1982.

Heggie, D. T., Skyring, G. W., O'Brien, G. W., Reimers, C., Herczeg, A., Moriarty, D. J. W., Burnett, W. C., and Milnes, A. R.: Organic carbon cycling and modern phosphorite formation on the East Australian continental margin: An overview, in: Phosphorite Research and Development, edited by: Notholt, A. J. G. and Jarvis, I., Geological Society, London, Special Publ., 52, 87–117, 1990.

Herlihy, M. and McCarthy, J.: Association of soil-test phosphorus with phosphorus fractions and adsorption characteristics, Nutr. Cycl. Agroecosys., 75, 79–90, 2006.

Hill, R. and Borman, D.: Estimating pastoral land use change for the Waikato region, in: Adding to the knowledge base for the nutrient manager, edited by: Currie, L. D. and Christensen, C. L., Occasional Report No. 24, Fertilizer and Lime Research Centre, Massey University, Palmerston North, New Zealand, p. 25, 2011.

Hinsinger, P.: Bioavailability of soil inorganic P in the rhizosphere as affected by root-induced chemical changes: A review, Plant Soil, 237, 173–195, 2001.

Hinsinger, P., Bengough, A. G., Vetterlein, D., and Young, I. M.: Rhizosphere: biophysics, biogeochemistry and ecological relevance, Plant Soil, 321, 117–152, 2009.

Howarth, R. W., Jensen, H. S., Marino, R., and Postma, H.: Transport to and processing of P in near-shore and oceanic waters, in: Phosphorus in the Global Environment – Transfers, Cycles and Management (Scope 54), edited by: Tiessen, H., Wiley, New York, NY, 323–345, 1995.

Huang, X. and Morris, J. T.: Distribution of phosphatase activity in marsh sediments along an estuarine salinity gradient, Mar. Ecol. Prog. Ser., 292, 75–83, 2005.

Husson, O.: Redox potential (Eh) and pH as drivers of soil/plant/microorganism systems: a transdisciplinary overview pointing to integrative opportunities for agronomy, Plant Soil, 362, 389–417, 2013.

Jahnke, R. A., Emerson, S. R., Roe, K. K., and Burnett, W. C.: The present day formation of apatite in Mexican continental margin sediments, Geochim. Cosmochim. Ac., 47, 259–266, 1983.

Jordan, T. E., Cornwell, J. C., Boynton, W. R., and Anderson, J. T.: Changes in phosphorus biogeochemistry along an estuarine salinity gradient: The iron conveyer belt, Limnol. Oceanogr., 53, 172–184, 2008.

Kizewski, F., Liu, Y.-T., Morris, A., and Hesterberg, D.: Spectroscopic approaches for phosphorus speciation in soils and other environmental systems, J. Environ. Qual., 40, 751–766, 2011.

Krajewski, K. P., van Cappellen, P., Trichet, J., Kuhn, O., Lucas, J., Martinalgarra, A., Prevot, L., Tewari, V. C., Gaspar, L., Knight, R. I., and Lamboy, M.: Biological processes and apatite formation in sedimentary environments, Eclog. Geol. Helvet., 87, 701–745, 1994.

Kurmies, B.: Zur Fraktionierung der Bodenphosphate, Die Phosphorsäure, 29, 118–149, 1972.

Lerman, A. and Wu, L.: Kinetics of global geochemical cycles, in: Kinetics of water-rock interactions, edited by: Brantley, S. L., Kubiki, J. D., and White, A. F., Springer, New York, 655–736, 2008.

Lindsay, W. L., Vlek, P. L. G., and Chien, S. H.: Phosphate minerals, in: Minerals in soil environments, edited by: Dixon, J. B. and Weed, S. B., Soil Sci. Soc. Am., Madison, 1089–1130, 1989.

Lovelock, C. E., Sorrell, B. K., Hancock, N., Hua, Q., and Swales, A.: Mangrove forest and soil development on a rapidly accreting shore in New Zealand, Ecosystems, 13, 437–451, 2010.

Lower, S. K.: Carbonate equilibria in natural waters – A Chem1 Reference Text, Simon Fraser University, June 1, 1999.

Lyons, G., Benitez-Nelson, C. R., and Thunell, R. C.: Phosphorus composition of sinking particles in the Guaymas Basin, Gulf of California, Limnol. Oceanogr., 56, 1093–1105, 2011.

Maher, W. A. and DeVries, M.: The release of phosphorus from oxygenated estuarine sediments, Chem. Geol., 112, 91–104, 1994.

Martens, C. S. and Harriss, R. C.: Inhibition of apatite precipitation in the marine environment by magnesium ions, Geochim. Cosmochim. Ac., 84, 621–625, 1970.

Morgan, M. F.: Chemical soil diagnosis by the universal soil testing system, Conn. Agric. Exp. Stn. Bull., 450, 579–628, 1941.

Morse, J. W. and Casey, W. H.: Ostwald processes and mineral paragenesis in sediments, Am. J. Sci., 288, 537–560, 1988.

Mortimer, C. H.: Chemical exchanges between sediments and water in Great Lakes – Speculations on probable regulatory mechanisms, Limnol. Oceanogr., 16, 387–404, 1971.

Murphy, J. and Riley, J. P.: A modified single solution method for the determination of phosphate in natural waters, Anal. Chim. Ac., 27, 31–36, 1962.

Murrmann, R. P. and Peech, M.: Effect of pH on labile and soluble phosphate in soils, Soil. Sci. Soc. Am. Proc., 33, 205–210, 1969.

Naidu, R., Syersy, J. K., Tillman, R. W., and Kirkman, J. H.: Effect of liming on phosphate sorption by acid soils, Eur. J. Soil Sci., 41, 165–175, 1990.

Nancollas, G. H., LoRe, M., Perez, L., Richardson, C., and Zawacki, S. J.: Mineral phases of calcium phosphate, Anat. Rec., 224, 234–241, 1989.

Noll, M. R., Szatkowski, A. E., and Magee, E. A.: Phosphorus fractionation in soil and sediments along a continuum from agricultural fields to nearshore lake sediments: Potential ecological impacts, J. Great Lakes Res., 35, 56–63, 2009.

Oh, Y.-M., Hesterberg, D. L., and Nelson, P. V.: Comparison of phosphate adsorption on clay minerals for soilless root media, Commun. Soil Sci. Plan., 30, 747–756, 1999.

Ostrofsky, M. L.: Determination of total phosphorus in lake sediments, Hydrobiologia, 696, 199–203, 2012.

Oxmann, J. F.: Technical Note: An X-ray absorption method for the identification of calcium phosphate species using peak-height ratios, Biogeosciences, 11, 2169–2183, 2014, http://www.biogeosciences.net/11/2169/2014/.

Oxmann, J. F. and Schwendenmann, L.: Quantification of octacalcium phosphate, authigenic apatite and detrital apatite in coastal sediments using differential dissolution and standard addition, Ocean Sci., 10, 571–585, 2014, http://www.ocean-sci.net/10/571/2014/.

Oxmann, J. F., Pham, Q. H., and Lara, R. J.: Quantification of individual phosphorus species in sediment: A sequential conversion and extraction method, Eur. J. Soil Sci., 59, 1177–1190, 2008.

Oxmann, J. F., Pham, Q. H., Schwendenmann, L., Stellman, J. M., and Lara, R. J.: Mangrove reforestation in Vietnam: The effect of sediment physicochemical properties on nutrient cycling, Plant Soil, 326, 225–241, 2010.

Paludan, C. and Morris, J. T.: Distribution and speciation of phosphorus along a salinity gradient in intertidal marsh sediments, Biogeochemistry, 45, 197–221, 1999.

Parfitt, R. L., Baisden, W. T., and Elliott, A. H.: Phosphorus inputs and outputs for New Zealand in 2001 at national and regional scales, J. R. Soc. N. Z., 38, 37–50, 2008.

Raimonet, M., Andrieux-Loyer, F., Ragueneau, O., Michaud, E., Kerouel, R., Philippon, X., Nonent, M., and Mémery, L.: Strong gradient of benthic biogeochemical processes along a macrotidal temperate estuary: Focus on P and Si cycles, Biogeochemistry, 115, 399–417, 2013.

Reddy, K. R. and DeLaune, R. D.: Biogeochemistry of wetlands: Science and applications, CRC Press, Boca Raton, 2008.

Reddy, K. R. and Sacco, P. D.: Decomposition of water hyacinth in agricultural drainage water, J. Environ. Qual., 10, 228–234, 1981.

Rengel, R.: Calcium, in: Encyclopedia of soil science, second edition, edited by: Lal, R., CRC Press, Boca Raton, 198–201, 2005.

Richardson, A. E., Barea, J., McNeill, A. M., and Prigent-Combaret, C.: Acquisition of phosphorus and nitrogen in the rhizosphere and plant growth promotion by microorganisms, Plant Soil, 321, 305–339, 2009.

Robertson, B. and Stevens, L.: Porirua Harbour: Intertidal fine scale monitoring 2008/09, Report prepared for Greater Wellington Regional Council, Wellington, New Zealand, 22 pp., 2009.

Ruttenberg, K. C.: Diagenesis and burial of phosphorus in marine sediments: Implications for the marine phosphorus budget, Ph.D. thesis, Yale Univ., New Haven, Connecticut, 1990.

Ruttenberg, K. C.: Development of a sequential extraction method for different forms of phosphorus in marine sediments, Limnol. Oceanogr., 37, 1460–1482, 1992.

Ruttenberg, K. C.: The global phosphorus cycle, in: Treatise on geochemistry, Vol. 8, edited by: Turekian, K. K. and Holland, D. J., Elsevier B. V., Amsterdam, 585–643, 2003.

Ruttenberg, K. C. and Berner, R. A.: Authigenic apatite formation and burial in sediments from non-upwelling continental margin environments, Geochim. Cosmochim. Ac., 57, 991–1007, 1993.

Schenau, S. J. and De Lange, G. J.: A novel chemical method to quantify fish debris in marine sediments, Limnol. Oceanogr., 45, 963–971, 2000.

Schenau, S. J., Slomp, C. P., and De Lange, G. J.: Phosphogenesis and active phosphorite formation in sediments from the Arabian Sea oxygen minimum zone, Mar. Geol., 169, 1–20, 2000.

Seitzinger, S. P.: The effect of pH on the release of phosphorus from Potomac estuary sediments: Implications for blue-green algal blooms, Estuar. Coast. Shelf. S., 33, 409–418, 1991.

Sharp, J. H., Culberson, C. H., and Church, T. M.: The chemistry of the Delaware estuary. General considerations, Limnol. Oceanogr., 27, 1015–1028, 1982.

Sheldon, R. P.: Ancient marine phosphorites, Annu. Rev. Earth Pl. Sc., 9, 251–284, 1981.

Slomp, C. P.: Phosphorus cycling in the estuarine and coastal zones: Sources, sinks, and Transformations, in: Treatise on estuarine and coastal science, Vol. 5, edited by: Wolanski, E. and McLusky, D. S., Academic Press, Waltham, 201–229, 2011.

Smyth, T. J. and Sanchez, P. A.: Effects of lime, silicate, and phosphorus applications to an Oxisol on phosphorus sorption and iron retention, Soil Sci. Soc. Am. J., 44, 500–505, 1980.

Sorensen, P. G. and Milne, J. R.: Porirua Harbour targeted intertidal sediment quality assessment, Report prepared for Greater Wellington Regional Council, Wellington, New Zealand, 71 pp., 2009.

Spiteri, C., Cappellen, P. V., and Regnier, P.: Surface complexation effects on phosphate adsorption to ferric iron oxyhydroxides along pH and salinity gradients in estuaries and coastal aquifers, Geochim. Cosmochim. Ac., 72, 3431–3445, 2008.

Sun, X. and Turchyn, A. V.: Significant contribution of authigenic carbonate to marine carbon burial, Nature Geosci., 7, 201–204, 2014.

Sundareshwar, P. V. and Morris, J. T.: Phosphorus sorption characteristics of intertidal marsh sediments along an estuarine salinity gradient, Limnol. Oceanogr., 44, 1693–1701, 1999.

Sutula, M., Bianchi, T. S., and McKee, B. A.: Effect of seasonal sediment storage in the lower Mississippi River on the flux of reactive particulate phosphorus to the Gulf of Mexico, Limnol. Oceanogr., 49, 2223–2235, 2004.

Swales, A., Bentley, S. J., Lovelock, C., and Bell, R. G.: Sediment processes and mangrove-habitat expansion on a rapidly-prograding muddy coast, New Zealand, Coastal Sediments '07, New Orleans, Louisiana, May 2007, 1441–1454, 2007.

Van Beusekom, J. E. E. and De Jonge, V. N.: Transformation of phosphorus in the Wadden Sea: Apatite formation, Deutsche Hydrographische Zeitschrift, 49, 297–305, 1997.

Van Cappellen, P. and Berner, R. A.: A mathematical model for the early diagenesis of phosphorus and fluorine in marine sediments; apatite precipitation, Am. J. Sci., 288, 289–333, 1988.

Van der Zee, C., Roevros, N., and Chou, L.: Phosphorus speciation, transformation and retention in the Scheldt estuary (Belgium/The Netherlands) from the freshwater tidal limits to the North Sea, Mar. Chem., 106, 76–91, 2007.

Vant, B. and Smith, P.: Trends in river water quality in the Waikato Region, 1987–2002, EW Technical Report 2004/02, Waikato Regional Council, Hamilton, New Zealand, 32 pp., 2004.

Yu, K., Böhme, F., Rinklebe, J., Neue, H-U, and Delaune, R. D.: Major biogeochemical processes in soils – A microcosm incubation from reducing to oxidizing conditions, Soil Sci. Soc. Am. J., 71, 1406–1417, 2007.